

# Transport properties of mixed $\text{CuAl}(\text{S}_{1-x}\text{Se}_x)_2$ as promising thermoelectric crystalline materials

A.H. Reshak <sup>a,b,\*</sup>

<sup>a</sup> New Technologies - Research Center, University of West Bohemia, Univerzitni 8, 306 14 Pilsen, Czech republic

<sup>b</sup> Center of Excellence Geopolymer and Green Technology, School of Material Engineering, University Malaysia Perlis, 01007 Kangar, Perlis, Malaysia

## ARTICLE INFO

### Article history:

Received 30 July 2014

Received in revised form

4 October 2014

Accepted 17 October 2014

Available online 22 October 2014

### Keywords:

A. Chalcogenides

Semiconductors

C. Ab initio calculations

D. Crystal structure

Transport properties

## ABSTRACT

The semi-classical Boltzmann theory as implemented in the BoltzTraP code is used to study the influence of substituting S by Se in the mixed  $\text{CuAl}(\text{S}_{1-x}\text{Se}_x)_2$  crystalline materials on the transport properties. The carrier concentration ( $n$ ), electrical conductivity ( $\sigma/\tau$ ), Seebeck coefficient ( $S$ ), electronic thermal conductivity ( $\kappa_e/\tau$ ), the electronic power factor ( $S^2\sigma/\tau$ ), and the figure of merit ( $ZT$ ) as a function of temperature at certain value of chemical potential are calculated. The carrier concentration, electrical conductivity, electronic thermal conductivity and the electronic power factor increase exponentially with increasing temperature.  $\text{CuAl}(\text{S}_{0.75}\text{Se}_{0.25})_2$  exhibits the highest  $n$ ,  $\sigma/\tau$ ,  $\kappa_e/\tau$  and  $S^2\sigma/\tau$  among these compounds along the whole temperature scale. We should emphasize that  $S$  is positive for all compounds which represents p-type concentration. At room temperature  $\text{CuAl}(\text{S}_{0.25}\text{Se}_{0.75})_2$  and  $\text{CuAl}(\text{S}_{0.5}\text{Se}_{0.5})_2$  exhibit  $ZT$  very close to unity, which implies that these materials could be good candidates for thermoelectric applications. The state-of-the-art full potential linear augmented plane wave (FP-LAPW) method is used to calculate the electronic band structure, density of states and energy gaps for  $\text{CuAl}(\text{S}_{1-x}\text{Se}_x)_2$ . The electron effective mass ratio ( $m_e^*/m_e$ ) and effective mass of the heavy holes ( $m_{hh}^*/m_e$ ) and light holes ( $m_{lh}^*/m_e$ ) around  $\Gamma$  point, the center of the BZ, for  $\text{CuAlS}_2$  and  $\text{CuAlSe}_2$  are calculated.

© 2014 Elsevier Ltd. All rights reserved.

## 1. Introduction

The conversion of sun's energy into electricity using photovoltaic cells open a new direction for the ecologically friendly production of electrical energy. Several materials have been tested for such photovoltaic applications. As a result, a notable progress in the photovoltaic field has been reported [1–4]. The ternary  $A^I B^{III} C_2^{VI}$  semiconducting compounds which crystallize in the chalcopyrite structure have received much attention in recent years [5–7]. They form a large group of semiconducting materials with diverse optical, electrical, and structural properties [8–15]. Ternary chalcopyrite appears to be promising candidate for solar-cell applications [16] and thermoelectric applications [17].

The specific  $A^I B^{III} C_2^{VI}$  chalcopyrites studied in this work used copper as the group XI element, aluminum as the group XIII element, and sulphur or selenium as the group XVI element. Since these compounds display large birefringence [18], they are potentially interesting as optical materials as well as semiconductors. We should emphasize that for the Cu containing chalcogenide

crystal, strong electron–phonon anharmonicity interacting with the highly polarizable cations a principal role begins to play [19]. So far, however, the trends of the coupling coefficients in these materials are not well understood. Here the first-principle calculations are used to predict enhancement of thermoelectric properties by substitution of S by Se. The band structure of  $A^I B^{III} C_2^{VI}$  chalcopyrites is influenced by intrinsic defects which exhibit additional trapping levels within the band gap of host materials, which leads to enhanced thermoelectric properties, as a consequence these materials turn to be suitable for optoelectronics, thermoelectric and photovoltaic applications. We would like to mention that we are not aware of calculations or experimental data for the thermoelectric properties for  $\text{CuAl}(\text{S}_{1-x}\text{Se}_x)_2$ . Therefore we thought it would be worthwhile to calculate the thermoelectric properties using the semi-classical Boltzmann theory as incorporated in BoltzTraP code [20].

## 2. Details of calculations

$\text{CuAl}(\text{S}_{1-x}\text{Se}_x)_2$  belongs to the group of ternary semiconducting compounds which are of great interest as solar cell materials [16] and nonlinear optical materials [21,22]. The state-of-the-art full potential linear augmented plane wave (FP-LAPW) method in a

\* Correspondence address: New Technologies - Research Center, University of West Bohemia, Univerzitni 8, 306 14 Pilsen, Czech republic. Fax: +420 386 361255. E-mail address: [maalidph@yahoo.com](mailto:maalidph@yahoo.com)

scalar relativistic version as embodied in the WIEN2k code [23] is used. This is an implementation of the density functional theory (DFT). Exchange and correlation potential is described in the generalized gradient approximation (GGA) of Perdew–Becke–Ernzerhof (PBE) [24], which is based on exchange–correlation energy optimization to calculate the total energy. The Kohn–Sham equations are solved using a basis of linear APWs. To achieve the total energy convergence, the basic functions in the interstitial regions are expanded up to  $R_{mt} \times K_{max}=7.0$  and inside the atomic spheres for the wave function. The potential and charge density in the muffin-tin (MT) spheres are expanded in spherical harmonics with  $l_{max}=8$  and nonspherical components up to  $l_{max}=6$ . In the interstitial region the potential and the charge density are represented by Fourier series up to  $G_{max}=20$  (a.u)<sup>-1</sup>. Self-consistency is obtained using 400  $\vec{k}$  points in the irreducible Brillouin zone (IBZ) for  $x=0.0$  and 1.0, while for  $x=0.25, 0.5$  and 0.75 a mesh of 600  $\vec{k}$  points was used. We have calculated the transport properties using 5000  $\vec{k}$  points in the IBZ. The self-consistent calculations are convergence since the total energy of the system is stable within  $10^{-5}$  Ry.

### 3. Results and discussion

#### 3.1. Salient features of the electronic band structures and density of states

We have used the semi-classical Boltzmann theory as implemented in the BoltzTraP code to study the influence of substituting S by Se in the mixed  $\text{CuAl}(\text{S}_{1-x}\text{Se}_x)_2$  on the transport properties. The calculated electronic band structure (Fig. 1) illustrated that substituting S by Se introduces extra bands in the valence and the conduction bands. The extra bands in the conduction band cause to push the conduction band minimum (CBM) towards Fermi level resulting in significant reduction in the energy gaps with increasing the content of Se. The values of the energy gaps are about 2.2 eV ( $\text{CuAlS}_2$ ), 1.9 eV ( $\text{CuAl}(\text{S}_{0.75}\text{Se}_{0.25})_2$ ), 1.7 eV ( $\text{CuAl}(\text{S}_{0.5}\text{Se}_{0.5})_2$ ), 1.5 eV ( $\text{CuAl}(\text{S}_{0.25}\text{Se}_{0.75})_2$ ) and 1.4 eV ( $\text{CuAlSe}_2$ ). In all cases the valence band maximum (VBM) and CBM are situated at  $\Gamma$  point, the center of the BZ. From the calculated electronic band structure one can obtain the values of the effective mass of electrons as well as heavy and light holes of  $\text{CuAlS}_2$  and  $\text{CuAlSe}_2$ , which are very important quantities for transport properties.

For further deep insight into the electronic structure of  $\text{CuAl}(\text{S}_{1-x}\text{Se}_x)_2$  we have calculated the partial density of states (PDOS). The calculated PDOS enables us to identify the angular momentum

character of the various structures. The PDOS of  $\text{CuAlS}_2$  is illustrated in Fig. 2(a) and (b); one can see that the VBM is mainly formed by Cu-d state with a small contribution from Cu-s/p, Al-s/p and S-p states. However the CBM is formed by Al-s/p and Cu-s/p states. The calculated energy gap is about 2.2 eV. Below Fermi level ( $E_F$ ) there exists a strong hybridization between Cu-s/p and Al-s/p states and between Cu-d and S-p states, while above Fermi level the Al-s state strongly hybridizes with Al-p state; also Al-p hybridizes with Cu-p state. The strong hybridization may lead to covalent bonds between the atoms.

Replacing 25% of S by Se leads to introduction of more bands in the VB and the CB; these bands are belong to Se-d, which shift the CBM towards  $E_F$ , resulting in energy gap's reduction by around 0.3 eV with respect to  $\text{CuAlS}_2$  (see Fig. 2(c)–(e)). The calculated energy band gap of  $\text{CuAl}(\text{S}_{0.75}\text{Se}_{0.25})_2$  is about 1.9 eV. It is clear that there is a strong hybridization between the states below and above  $E_F$ , for instance around  $-15.0$  eV, Cu-s/p hybridized with Al-p and also Se-s with S-s. In the energy region between  $-7.0$  eV and  $E_F$ , Cu-s hybridized with Al-p, Al-p with Cu-p and Se-p with S-p. Whereas above  $E_F$ , Cu-s/p hybridized with Se-d; also Cu-p hybridized with Al-p and Se-p states.

The PDOS of  $\text{CuAl}(\text{S}_{0.5}\text{Se}_{0.5})_2$  is represented in Fig. 2(f)–(h); one can see that they are quite similar to those of  $\text{CuAl}(\text{S}_{0.75}\text{Se}_{0.25})_2$  in the matter of peak positions and the hybridizations except that the CBM shifts towards  $E_F$  by around 0.2 eV with respect to  $\text{CuAl}(\text{S}_{0.75}\text{Se}_{0.25})_2$  leading to reduction of the energy band gap to 1.7 eV.

Substituting 75% of S by Se led to pushing the CBM further towards  $E_F$  resulting in a band gap of about 1.5 eV; the PDOS of  $\text{CuAl}(\text{S}_{0.25}\text{Se}_{0.75})_2$  is shown in Fig. 2(i)–(k). Finally substituting all S atoms by Se to form the end compound  $\text{CuAlSe}_2$  causes to further shifts of the CBM towards  $E_F$  to yield a band gap of about 1.4 eV; the PDOS of  $\text{CuAlSe}_2$  is represented in Fig. 2(l) and (m). These figures suggest that there exists a strong hybridization between the states below and above  $E_F$ .

#### 3.2. Effective mass

It is further interesting to study the effective masses of electrons and holes, which are important for the excitonic compounds. To obtain accurate values of the effective mass one needs to calculate the curvature of the CBM and the VBM in the vicinity of  $\Gamma$  point. At  $\Gamma$  point, the effective mass can be obtained through a simple parabolic fitting using the definition of effective mass as a second derivative of energy band with respect to the wave vector,  $k$ :

$$\frac{1}{m^*} = \frac{\partial^2 E(k)}{\hbar^2 \partial k^2} \quad (1)$$

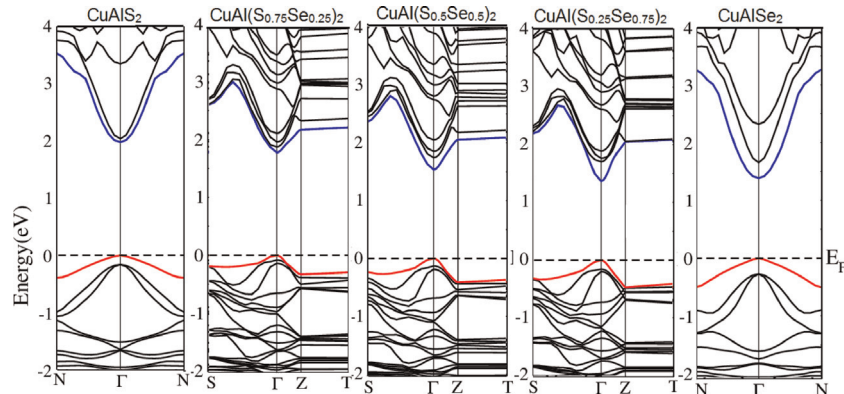


**Fig. 1.** Calculated electronic band structure for  $\text{CuAl}(\text{S}_{1-x}\text{Se}_x)_2$  used to calculate the electron effective mass ratio ( $m_e^*/m_e$ ), effective mass of the heavy holes ( $m_{hh}^*/m_e$ ) and light holes ( $m_{lh}^*/m_e$ ), around  $\Gamma$  point the center of the BZ. The larger the band curvature, the smaller the effective mass.

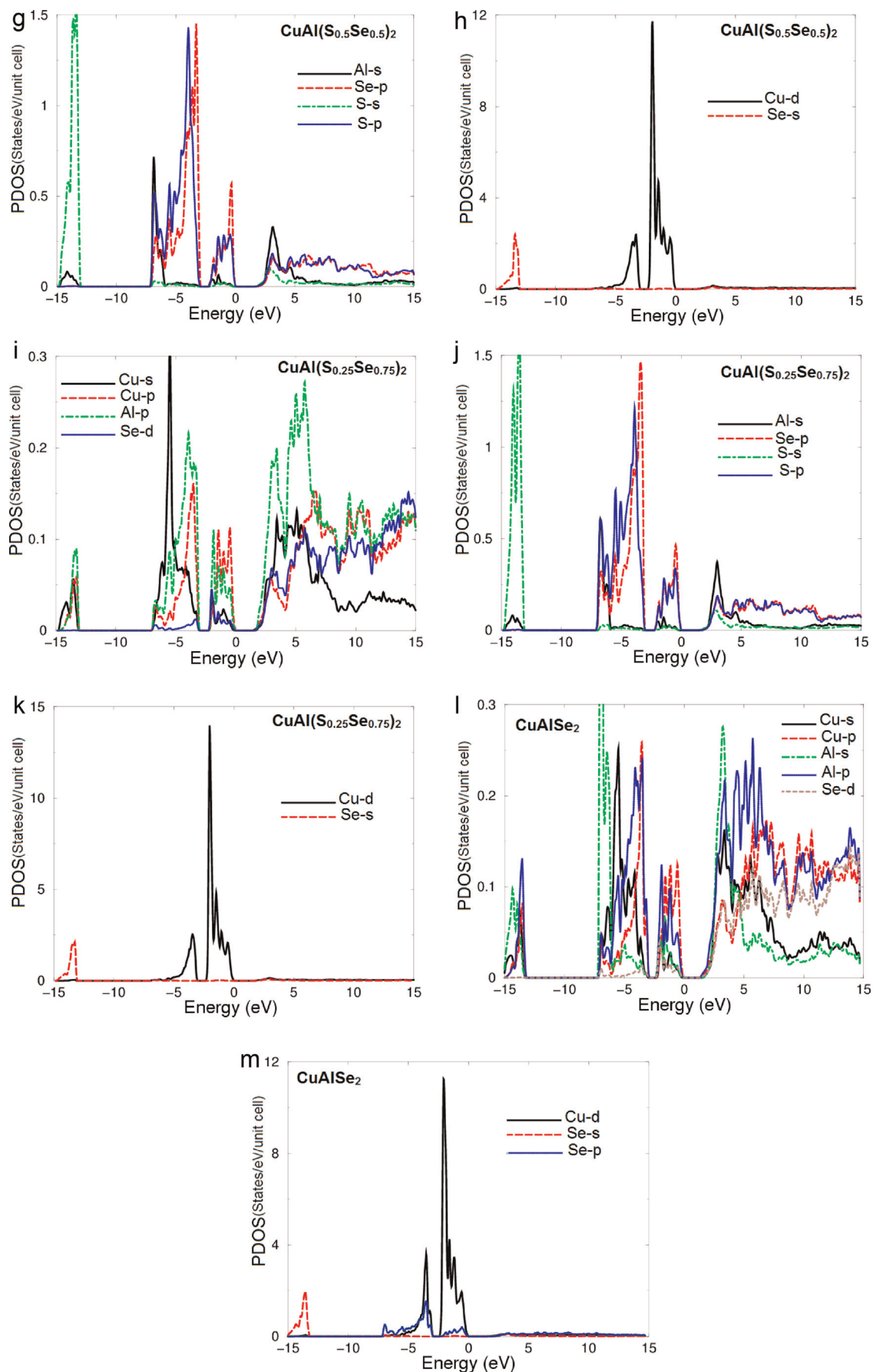


Fig. 2. Calculated partial density of states (states/eV/unit cell) for  $\text{CuAl}(\text{S}_{1-x}\text{Se}_x)_2$ .

**Table 1**

Calculated the electron effective mass ratio ( $m_e^*/m_e$ ), effective mass of the heavy holes ( $m_{hh}^*/m_e$ ) and light holes ( $m_{lh}^*/m_e$ ), around  $\Gamma$  point the center of the BZ for CuAlS<sub>2</sub> and CuAlSe<sub>2</sub>.

Compound	$m_e^*/m_e$	$m_{hh}^*/m_e$	$m_{lh}^*/m_e$
CuAlS <sub>2</sub>	0.007058	0.036038	0.018401
CuAlSe <sub>2</sub>	0.006624	0.025585	0.013020

We can calculate the curvature of the VBM using the following approach: if the spin–orbit interaction were neglected, the top of the valence band would have a parabolic behavior; this implies that the highest valence bands are parabolic in the vicinity of the point  $\Gamma$ . In this work, CuAlS<sub>2</sub> and CuAlSe<sub>2</sub> compounds satisfy this parabolic condition of the maximum of valence band at the point  $\Gamma$ . From the electronic band structures (Fig. 1) we have calculated the electron effective mass ratio ( $m_e^*/m_e$ ) and effective mass of the heavy holes ( $m_{hh}^*/m_e$ ) and light holes ( $m_{lh}^*/m_e$ ) around  $\Gamma$  point, the center of the BZ, for CuAlS<sub>2</sub> and CuAlSe<sub>2</sub> compounds. These values are listed in Table 1. From Table 1 we note that the electron effective mass for CBM is very small because of the high curvature of the CBM around  $\Gamma$ , and this effective mass is isotropic so that the constant energy surfaces are spheres. The effective masses for heavy and light holes are higher than that of the electrons because the VBM and the next VB around  $\Gamma$  have less curvatures than that of the CBM (see Fig. 1). The condition  $n_e = n_h$  for intrinsic semiconductors is used to determine the position of the Fermi levels ( $E_F$ ) for electrons and holes within the band gap. If the band curvatures of the valence and conduction bands are the same, then their effective masses are of the same magnitude and  $E_F$  lies at mid-gap. We derive in this section the general result for the placement of  $E_F$  when  $m_e^* \neq m_h^*$ . If  $m_e^* = m_h^*$  we obtain the simple result that  $E_F^e = E_g/2$  which says that the Fermi level lies in the middle of the energy gap (Fermi level for  $n_e$  is  $E_F^e$  and for  $n_h$  is  $E_F^h$ ). However, if the masses are not equal,  $E_F$  will lie closer to the band edge with low curvature, thereby enhancing the Boltzmann factor term in the thermal excitation process, to compensate for the lower density of states for the higher curvature band.

We can say in some approximate way that an electron in a solid moves as if it were a free electron but with an effective mass  $m^*$  rather than a free electron mass. The larger the band curvature, the smaller the effective mass. From the electronic band structure diagram (Fig. 1) one would expect that hole carriers could be thermally excited to a second band at the  $\Gamma$  point. At room temperature, these  $\Gamma$  point hole carriers contribute significantly to the transport properties.

### 3.3. Transport properties

The semi-classical Boltzmann theory as incorporated in BoltzTraP code [20] is used to calculate the transport properties of CuAl(S<sub>1-x</sub>Se<sub>x</sub>)<sub>2</sub>. We should emphasize that in the BoltzTraP code the relaxation time  $\tau$  is taken as a constant. It is important to mention that the BoltzTraP code has proven to be a very efficient technique for calculating the electronic transport properties [25], namely the carrier concentration ( $n$ ), electrical conductivity ( $\sigma/\tau$ ), Seebeck coefficient ( $S$ ), electronic thermal conductivity ( $\kappa_e/\tau$ ), the electronic power factor ( $S^2\sigma/\tau$ ), and the figure of merit ( $ZT$ ) as a function of temperature at certain value of chemical potential.

Usually the combination of the high mobility ( $\mu$ ) and reasonable carrier concentration ( $n$ ) gives better thermoelectric properties. For metals the carrier concentration is essentially independent of temperature, while  $\mu$  is temperature dependent. In contrast,  $n$  for semiconductors is highly temperature dependent in the intrinsic regime and  $\mu$  is relatively less temperature

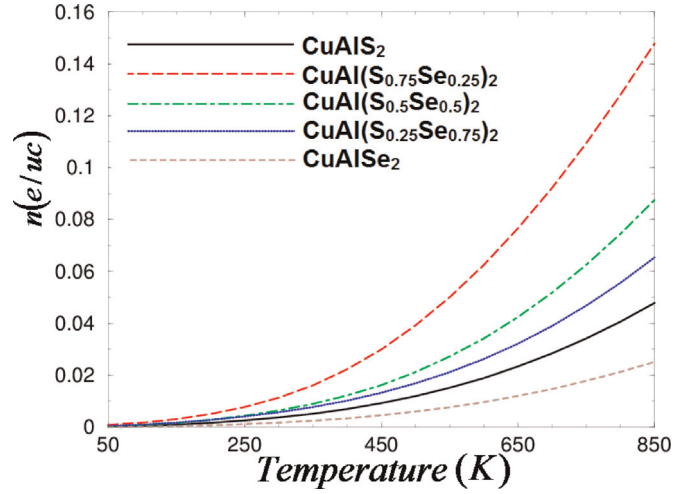


Fig. 3. Calculated carrier concentration ( $n$ ) in  $e/uc$  for CuAl(S<sub>1-x</sub>Se<sub>x</sub>)<sub>2</sub>.

dependent. The carrier concentration ( $n$ ) versus temperature at certain chemical potential value is calculated for CuAl(S<sub>1-x</sub>Se<sub>x</sub>)<sub>2</sub> with  $x=0.0, 0.25, 0.5, 0.75$  and  $1.0$  as shown in Fig. 3. The carrier concentration is zero at 50–100 K then it increases exponentially with increasing temperature. As a remarkable finding we observe that CuAl(S<sub>0.75</sub>Se<sub>0.25</sub>)<sub>2</sub> exhibits rapid increase and the highest carrier concentration among compounds which show the same tendency. The observed highest carrier concentration for CuAl(S<sub>0.75</sub>Se<sub>0.25</sub>)<sub>2</sub> could be attributed to the fact that substituting 0.25 of S by Se cause to reaching the highest value of the carrier concentration along the temperature range. We should emphasize that the electronegativities for S and Se atoms are almost the same, therefore there is no electronegativity influence with substituting S by Se because the electronegativity difference is very small. The values of the carrier concentration of CuAl(S<sub>1-x</sub>Se<sub>x</sub>)<sub>2</sub> with  $x=0.0, 0.25, 0.5, 0.75$  and  $1.0$  compounds at 850 K are listed in Table 2.

The electrical conductivity ( $\sigma = ne\mu$ ) is related to the density of charge carriers ( $n$ ) and their mobility ( $\mu_e = e\tau_e/m_e^*$  and  $\mu_h = e\tau_h/m_h^*$ ) which shows that materials with small effective masses have high mobility. Therefore, for better thermoelectric properties we should reach a good combination of high mobility and reasonable carrier concentration. Therefore, to design good thermoelectric device, the materials should have high electrical conductivity to reduce the Joule heating effect [26]. Fig. 4 exhibits the calculated electrical conductivity ( $\sigma/\tau$ ) as a function of temperature at a certain value of chemical potential. It is clear that with increasing temperature the electrical conductivity increases exponentially; the rapid increase with increasing the temperature is due to enhanced the charge carrier concentration and the mobility of the carriers in the conduction band. As we show in Fig. 3, CuAl(S<sub>0.75</sub>Se<sub>0.25</sub>)<sub>2</sub> possesses the highest carrier concentration; here (in Fig. 4) CuAl(S<sub>0.75</sub>Se<sub>0.25</sub>)<sub>2</sub> shows the highest electrical conductivity which confirms that

**Table 2**

Calculated carrier concentration ( $n$ ) in ( $e/uc$ ),  $(\sigma/\tau)10^{18}(\Omega\text{ms})^{-1}$  and  $(\kappa_e/\tau)10^{14}(W/m\text{ks})$  at 850 K for CuAl(S<sub>1-x</sub>Se<sub>x</sub>)<sub>2</sub>.

Compound	$n$ in ( $e/uc$ )	$(\sigma/\tau)10^{18}(\Omega\text{ms})^{-1}$	$(\kappa_e/\tau)10^{14}(W/m\text{ks})$
CuAlS <sub>2</sub>	0.048	5.2	4.5
CuAl(S <sub>0.75</sub> Se <sub>0.25</sub> ) <sub>2</sub>	0.146	7.0	4.8
CuAl(S <sub>0.5</sub> Se <sub>0.5</sub> ) <sub>2</sub>	0.086	4.6	3.5
CuAl(S <sub>0.25</sub> Se <sub>0.75</sub> ) <sub>2</sub>	0.065	4.5	3.9
CuAlSe <sub>2</sub>	0.025	3.7	3.2

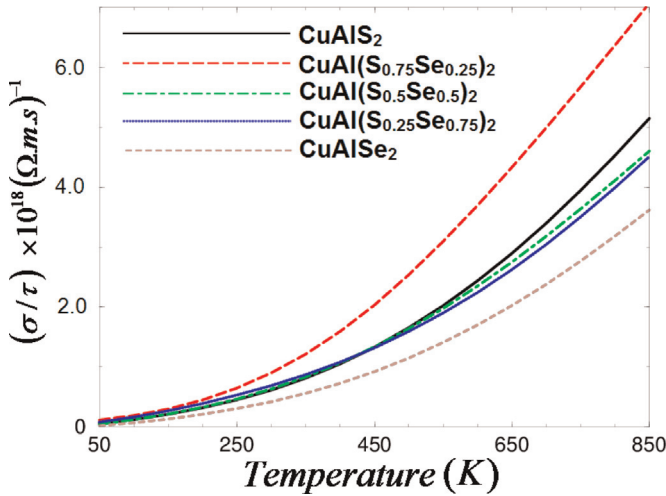


Fig. 4. Calculated electrical conductivity ( $\sigma/\tau$ ) in  $10^{18}(\Omega \text{ m} \cdot \text{s})^{-1}$  for  $\text{CuAl}(\text{S}_{1-x}\text{Se}_x)_2$ .

substituting 0.25 of S by Se leads to the highest carrier concentration and hence the highest electrical conductivity according to  $\sigma = ne\mu$ . We would like to mention that at low temperature (50 K) all  $\text{CuAl}(\text{S}_{1-x}\text{Se}_x)_2$  compounds exhibit zero electrical conductivity. When we substitute half number of S atoms by Se we notice that  $\sigma/\tau$  of  $\text{CuAl}(\text{S}_{0.5}\text{Se}_{0.5})_2$  drops below the values of  $\text{CuAl}(\text{S}_{0.75}\text{Se}_{0.25})_2$  and  $\text{CuAlS}_2$ , while it is above those of  $\text{CuAl}(\text{S}_{0.25}\text{Se}_{0.75})_2$  and  $\text{CuAlSe}_2$  along the temperature scale. Thus, increasing Se content causes reduced  $\sigma/\tau$ . It is important to mention here that the fluctuation in the values of  $\sigma/\tau$  with changing content of Se atoms is attributed to the mobility, the effective masses and the concentration of the charge carrier. The values of the electrical conductivity of  $\text{CuAl}(\text{S}_{1-x}\text{Se}_x)_2$  with  $x=0.0, 0.25, 0.5, 0.75$  and 1.0 compounds at 850 K are listed in Table 2.

Seebeck coefficients also called as thermopower, which are usually use to determine the majority carrier type, have an inverse relationship with electrical conductivity. Here we plot the Seebeck coefficients of  $\text{CuAl}(\text{S}_{1-x}\text{Se}_x)_2$  compounds as a function of temperature. Following Fig. 5, at low temperature around 50 K the end compound  $\text{CuAlSe}_2$  exhibits the highest value of Seebeck coefficient and  $\text{CuAl}(\text{S}_{0.5}\text{Se}_{0.5})_2$  compound shows the next highest value among the others. With a little increase in the temperature both of  $\text{CuAlSe}_2$  and  $\text{CuAl}(\text{S}_{0.5}\text{Se}_{0.5})_2$  exhibit a valley which has a minimum at 75 K. Beyond 100 K the Seebeck coefficient of all compounds

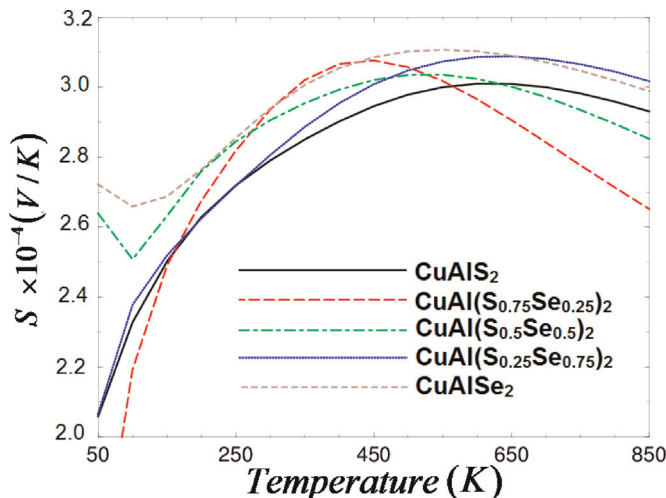


Fig. 5. Calculated Seebeck coefficient ( $S$ ) for  $\text{CuAl}(\text{S}_{1-x}\text{Se}_x)_2$ .

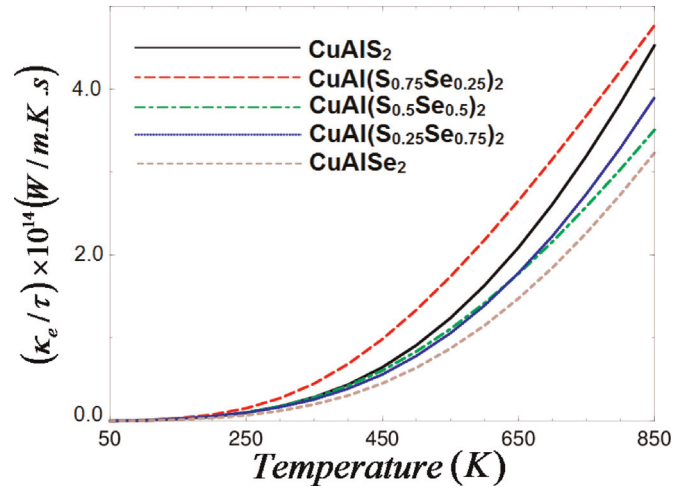


Fig. 6. Calculated electronic thermal conductivity ( $\kappa_e/\tau$ ) for  $\text{CuAl}(\text{S}_{1-x}\text{Se}_x)_2$  in  $10^{14}(\text{W}/\text{m} \cdot \text{K} \cdot \text{s})$ .

increases with temperature to reach the maximum values at 650 K ( $\text{CuAlS}_2$ ), 400 K ( $\text{CuAl}(\text{S}_{0.75}\text{Se}_{0.25})_2$ ), 500 K ( $\text{CuAl}(\text{S}_{0.5}\text{Se}_{0.5})_2$ ), 650 K ( $\text{CuAl}(\text{S}_{0.25}\text{Se}_{0.75})_2$ ) and 500 K ( $\text{CuAlSe}_2$ ). Beyond these maximums, further increases in the temperature cause significant reduction in the Seebeck coefficient of all compounds especially for  $\text{CuAl}(\text{S}_{0.5}\text{Se}_{0.5})_2$ . We can see that all materials exhibit high Seebeck coefficient at room temperature. We should emphasize that the Seebeck coefficient is positive for all compounds which represents the p-type concentration. In general increasing the temperature causes enhanced hole doping in  $\text{CuAl}(\text{S}_{1-x}\text{Se}_x)_2$ .

The thermal conductivity has contributions from the lattice and electrons ( $\kappa = \kappa_l + \kappa_e$ ). the BoltzTraP code calculates only the electronic part ( $\kappa_e$ ). The electronic thermal conductivity ( $\kappa_e/\tau$ ) of the investigated compounds as a function of temperature is presented in Fig. 6. The electronic thermal conductivity can be estimated from the electrical conductivity  $\sigma$  by using the Wiedemann–Franz relation. The electronic thermal conductivity is zero for all compounds at low temperature between 50 and 200 K, and then increases exponentially with increasing the temperature. It is clear that  $\text{CuAl}(\text{S}_{0.75}\text{Se}_{0.25})_2$  shows the highest  $\kappa_e/\tau$  along the temperature scale that is attributed to the fact that  $\text{CuAl}(\text{S}_{0.75}\text{Se}_{0.25})_2$  possess the highest carrier concentration (Fig. 3) and the highest electrical conductivity (Fig. 4) which again confirms our previous finding that substituting 0.25 of S by Se leads to the highest carrier concentration and hence the highest electrical conductivity according to  $\sigma = ne\mu$ . In the absence of any calculations or measurements of the lattice thermal conductivity it is difficult to say which compound will have the largest figure of merit (FOM). The values of the electronic thermal conductivity of  $\text{CuAl}(\text{S}_{1-x}\text{Se}_x)_2$  with  $x=0.0, 0.25, 0.5, 0.75$  and 1.0 compounds at 850 K are listed in Table 2.

Now let us turn our concern to study the electronic power factor ( $S^2\sigma/\tau$ ); it is well-known that  $S^2\sigma/\tau$  is a keynote quantity for measuring transport properties. Fig. 7 illustrated  $S^2\sigma/\tau$  as a function of temperature; one can see that at 50 K all compounds exhibit zero  $S^2\sigma/\tau$ , which then rapidly increases with increasing the temperature. It is clear that  $\text{CuAl}(\text{S}_{0.75}\text{Se}_{0.25})_2$  shows the highest  $S^2\sigma/\tau$  among these materials that is attributed to the fact that  $\text{CuAl}(\text{S}_{0.75}\text{Se}_{0.25})_2$  has the highest  $n$  and hence  $\sigma$ . The low Se content is optimal in improving  $\sigma/\tau$ , and  $S^2\sigma/\tau$ , that is attributed to the surfactant effects of Se. We find a huge reduction in  $S^2\sigma/\tau$  with increasing Se content. In general we expect that increasing the temperature should yield a high power factor.

In the last few years thermoelectric power generation (TPG) has become an increasingly popular technology for waste heat

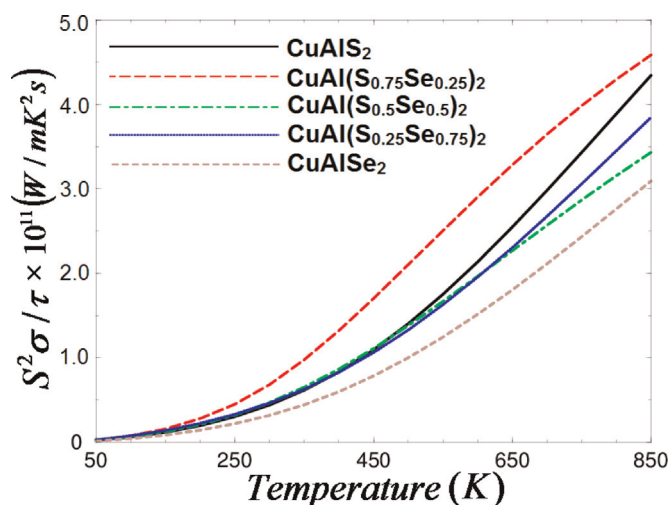


Fig. 7. Calculated electronic power factor ( $S^2\sigma/\tau$ ) for  $\text{CuAl}(\text{S}_{1-x}\text{Se}_x)_2$ .

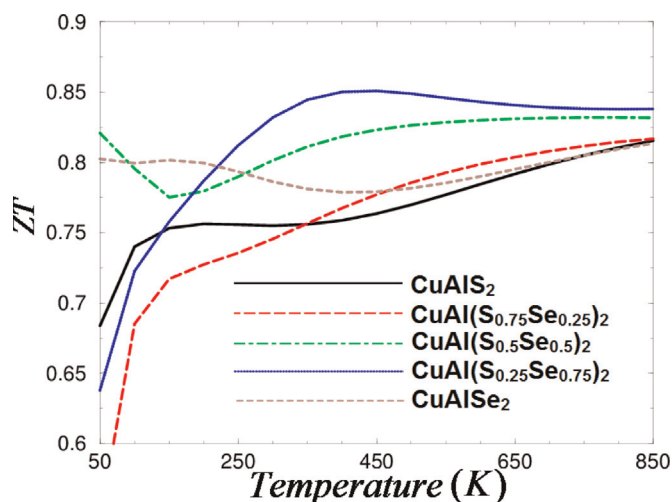


Fig. 8. Calculated figure of merit ( $ZT$ ) for  $\text{CuAl}(\text{S}_{1-x}\text{Se}_x)_2$ .

recovery. The efficiency of TPG is essential in determining how practical this technology is in real applications. The efficiency of TPG is calculated using the dimensionless figure of merit ( $ZT$ );  $ZT = S^2\sigma T/\kappa_e$ , where  $S$  is the Seebeck coefficient,  $\sigma$  is the electrical conductivity,  $T$  is the absolute temperature, and  $\kappa_e$  is the electronic thermal conductivity. It is well known that higher figure of merit leads to higher efficiency, but increasing  $ZT$  in bulk semiconductors ( $ZT \leq 1$ ) has proven to be difficult because of the variables' interdependence; a reduction in thermal conductivity typically leads to a reduction in electrical conductivity, and  $S$  has an inverse relationship with  $\sigma$ . Fig. 8, illustrates  $ZT$  as a function of temperature. It is clear that at low temperature around 50 K,  $\text{CuAl}(\text{S}_{0.5}\text{Se}_{0.5})_2$  shows the highest  $ZT$ . Figure of merit depends on the Seebeck coefficient; thus for a good thermoelectric device we need a large Seebeck coefficient with small thermal conductivity so the temperature gradient could be maintained. Materials having  $ZT$  about unity or greater than unity are considered excellent candidates for thermoelectric devices [27,28]. From Fig. 8 one can see that at room temperature  $ZT$  is very close to unity, which implies that  $\text{CuAl}(\text{S}_{0.25}\text{Se}_{0.75})_2$  and  $\text{CuAl}(\text{S}_{0.5}\text{Se}_{0.5})_2$  could be good candidates for thermoelectric applications. This is attributed to the fact that at room temperature the Seebeck coefficient gives high values (Fig. 5) and the electronic thermal conductivity has minimum values (Fig. 6). Both of  $\text{CuAl}(\text{S}_{0.25}\text{Se}_{0.75})_2$  and  $\text{CuAl}(\text{S}_{0.5}\text{Se}_{0.5})_2$

maintain this behavior till 450 K. Beyond this temperature  $ZT$  decreases due to the sharp increase in the electronic thermal conductivity (Fig. 6).

To the best of our knowledge, there are no previous experimental or theoretical data for the thermoelectric properties of the investigated materials available in literature to make a meaningful comparison. We would like to mention here that in Ref. [17] the authors have calculated the thermoelectric properties, using the FPLAPW method and BoltzTraP code, of some chalcopyrite structure materials whose thermoelectric properties are known experimentally and they find very good agreement with the experimental data. Since we use the same methodology mentioned in Ref. [17], thus we believe that our calculations reported in this paper would produce very accurate and reliable results.

#### 4. Conclusions

In summary, based on the density functional theory, the state-of-the-art full potential linear augmented plane wave (FPLAPW) method is used to calculate the total energy of the mixed  $\text{CuAl}(\text{S}_{1-x}\text{Se}_x)_2$  compounds. From the obtained electronic band structure, energy gaps of  $\text{CuAl}(\text{S}_{1-x}\text{Se}_x)_2$  compounds are obtained. Also the electron effective mass ratio ( $m_e^*/m_e$ ) and effective mass of the heavy holes ( $m_{hh}^*/m_e$ ) and light holes ( $m_{lh}^*/m_e$ ), around  $\Gamma$  point, the center of the BZ, for  $\text{CuAlS}_2$  and  $\text{CuAlSe}_2$  are calculated. Based on the above calculations the transport properties are obtained using the semi-classical Boltzmann theory as implemented in the BoltzTraP code. We demonstrated the influence of substituting S by Se on the electronic band structure, density of states, the effective masses and hence the transport properties. We found that the carrier concentration, electrical conductivity, thermal conductivity and the electronic power factor increase exponentially with increasing temperature. The compound  $\text{CuAl}(\text{S}_{0.75}\text{Se}_{0.25})_2$  exhibits the highest carrier concentration, electrical conductivity, thermal conductivity and the electronic power factor among these compounds. The observed highest carrier concentration, electrical conductivity, thermal conductivity and the electronic power factor for  $\text{CuAl}(\text{S}_{0.75}\text{Se}_{0.25})_2$  could be attributed to the fact that substituting 0.25 of S by Se causes reaching the highest value of the carrier concentration along the temperature range. Thus, the  $\text{CuAl}(\text{S}_{0.75}\text{Se}_{0.25})_2$  compound shows high electrical conductivity and electronic power factor. We have obtained positive Seebeck coefficient for all compounds which represents p-type concentration. At room temperature both  $\text{CuAl}(\text{S}_{0.25}\text{Se}_{0.75})_2$  and  $\text{CuAl}(\text{S}_{0.5}\text{Se}_{0.5})_2$  possess figure of merit very close to unity, which implies that these materials could be good candidates for thermoelectric applications.

#### Acknowledgements

The result was developed within the CENTEM Project, reg. no. CZ.1.05/2.1.00/03.0088, co-funded by the ERDF as part of the Ministry of Education, Youth and Sports OP RDI program. Computational resources were provided by MetaCentrum (LM2010005) and CERIT-SC (CZ.1.05/3.2.00/08.0144) infrastructures.

#### References

- [1] S. Guenes, H. Neugebauer, N.S. Sariciftci, Chem. Rev. 107 (2007) 1324.
- [2] H. Hoppe, N.S. Sariciftci, J. Mater. Res. 19 (2004) 1924–19 (2004).
- [3] Grätzel Michael, Acc. Chem. Res. 42 (11) (2009) 1788–1798.
- [4] M.A. Contreras, B. Egaas, K. Ramanathan, J. Hiltner, A. Swartzlander, F. Hasoon, R. Noufi, Prog. Photovolt. 7 (1999) 311.

- [5] Balzarotti, A. (1987), in: Ternary and Multinary compounds-Proceedings of the 7th International Conference on Ternary and Multinary Compounds, (Eds.), S. K. Deb and Z. Zunger (Materials Research Society, Pittsburgh, PA), p. 333.
- [6] G.E. Jaffe, A. Zunger, Phys. Rev. B 28 (5822v) (1983), G.E. Jaffe, A. Zunger, Phys. Rev. B 29 (1882) (1984).
- [7] C. Rincon, C. Bellabarba, Phys. Rev. B 33 (1986) 7160.
- [8] E. Parthe, Crystal Chemistry of Tetrahedral Structures, Gordon and Breach, New York, 1964.
- [9] N.A. Goryunova, The Chemistry of Diamond-Like Semiconductors, Chapman and Hall, New York, 1965.
- [10] J.L. Shay, J.H. Wernick, Ternary Chalcopyrite Semiconductors: Growth, Electronic Properties and Applications, Pergamon, Oxford, 1974.
- [11] U. Kaufmann, J. Schneider, in: J. Treusch (Ed.), Festkörperprobleme XIV, Vieweg, Braunschweig, 1974, p. 229.
- [12] Wagner, in: J.O. Pankove (Ed.), in Electroluminescence, Springer, Berlin, 1977, p. 171.
- [13] A. Mackinnon, in: J. Treusch (Ed.), Festkörperprobleme XXI, Vieweg, Dortmund, 1981, p. 149.
- [14] A. Miller, A. Mackinnon, D. Weaire, in: H. Ehrenreich, F. Seitz, D. Turubull (Eds.), solid State Physics, vol.36, Academic, New York, 1981.
- [15] B.R. Pamplin, T. Kiyosawa, K. Mastumoto, Prog. Cryst. Growth Charact. 1 (1979) 331.
- [16] L.L. Kazmerski, Nuovo Cimento D2 103 (1983).
- [17] David Parker, David J. Singh, Phys. Rev. B 85 (12) (2012) 125209.
- [18] A.H. Reshak, V. Kityk, S. Auluck, J. Phys. Chem. B 114 (2010) 16705–16712.
- [19] E. Al-Harbi, A. Wojciechowski, N. AlZayed, O.V. Parasyuk, E. gondok, P. Armatys, A.M. El-Naggar, I.V. Kityk, P. Karasinski, Spectrochim. Acta A V.111 (2013) 142–149.
- [20] K. Georg, H. Madsen, David J. Singh, Comput. Phys. Commun. 175 (2006) 67–71.
- [21] G.D. Boyd, H. Kasper, J.H. McFee, IEEE J. Quantum Electron. (1971)563.
- [22] D.S. Chemla, P.J. Kupcek, D.S. Robertson, R.C. Smith, Opt. Commun. 3 (1971) 29.
- [23] P. Blaha, K. Schwarz, G.K.H. Madsen, D. Kvasnicka, J. Luitz, WIEN2k, An Augmented Plane Wave Plus Local Orbitals Program For Calculating Crystal Properties, Vienna University of Technology, Austria, 2001.
- [24] J.P. Perdew, S. Burke, M. Ernzerhof, Phys. Rev. Lett. 77 (1996) 3865.
- [25] K. Nouneh, A.H. Reshak, S. Auluck, I.V. Kityk, R. Viennois, S. Benet, S. Charar, J. Alloys Compd. 437 (2007) 39–46.
- [26] H.A.R. Aliabad, M. Ghazanfari, I. Ahmad, M.A. Saeed, Comput. Mater. Sci. 65 (2012) 509–519.
- [27] O. Rabin, L. Yu-Ming, M.S. Dresselhaus, Appl. Phys. Lett. 79 (2001) 81–83.
- [28] T. Takeuchi, Mater. Trans. 50 (2009) 2359–2365.